Strong size-dependent stress relaxation in electrospun polymer nanofibers

Matthew C. Wingert,[1] Zhang Jiang,[2] Renkun Chen,[1,a)] and Shengqiang Cai[1,a)]
[1]*Department of Mechanical and Aerospace Engineering, University of California, San Diego, La Jolla, California 92093, USA*
[2]*X-ray Science Division, Argonne National Laboratory, Argonne, Illinois 60439, USA*

Electrospun polymer nanofibers have garnered significant interest due to their strong size-dependent material properties, such as tensile moduli, strength, toughness, and glass transition temperatures. These properties are closely correlated with polymer chain dynamics. In most applications, polymers usually exhibit viscoelastic behaviors such as stress relaxation and creep, which are also determined by the motion of polymer chains. However, the size-dependent viscoelasticity has not been studied previously in polymer nanofibers. Here, we report the first experimental evidence of significant size-dependent stress relaxation in electrospun Nylon-11 nanofibers as well as size-dependent viscosity of the confined amorphous regions. In conjunction with the dramatically increasing stiffness of nano-scaled fibers, this strong relaxation enables size-tunable properties which break the traditional damping-stiffness tradeoff, qualifying electrospun nanofibers as a promising set of size-tunable materials with an unusual and highly desirable combination of simultaneously high stiffness and large mechanical energy dissipation.

I. INTRODUCTION

One striking feature of electrospun[1–4] polymer nanofibers is their strong size-dependent material properties, which can change many times that of their bulk values. Widespread interest in polymer nanofibers stems from studies showing that the moduli[5] and thermal conductivities[6] of semi-crystalline polymer nanofibers are strongly dependent on the fiber diameter, specifically in the 100 nm to 1 μm range.[1,5,7–14] Further studies have expanded our understanding of the mechanical and thermal properties in these nanoscale fibers, such as strength, toughness, and glass transition and melting temperatures.[13,15,16] These various observed mechanical and thermal behaviors are closely associated with the dynamics of polymer chains within the nanofiber. Quite recently, it was found that along with the modulus, the yield strength and toughness of individual semi-crystalline nanofibers also increased significantly as diameter decreased.[13] This increase in toughness was unexpected as it opposes the classical tradeoff between strength and toughness in bulk materials,[17] such as bulk polymers and metals. Consequently, a diverse range of applications for polymer nanofibers have been proposed, such as in military protective clothing,[18] nanosensors,[3,19] tissue engineering scaffolding,[20–22] and thermal packaging.[23]

Toughness of polymers mainly comes from two molecular scale processes: breaking of polymer chains and sliding between polymer chains which macroscopically manifests as viscoelasticity.[24,25] In electrospun semi-crystalline fibers, size-dependent modulus, strength, and toughness have been attributed to increased polymer chain alignment in the amorphous domain and decrease of crystallinity.[13] Furthermore, thermal studies on nanofibers have observed size-dependent dissipative effects, such as modulus softening upon heating[26] and decreased glass transition[15] and melting[16] temperatures with diameter reduction. These disparate observations indirectly suggest that any mechanical relaxation should also exhibit size-dependent behavior, which has not been investigated in previous studies on the mechanical properties of individual electrospun polymer fibers.

Many size-dependent properties of polymer nanofibers have been recently discovered and are believed to stem from the confinement of polymer chains near surfaces and in amorphous regions,[5,10,15,27] the reduction of polymer chain entanglement,[16,28] and the increase of the alignment of polymer chains. To explain the observed stress-relaxation in the electrospun Nylon-11 fibers with small diameters in our experiments, we propose that the increased orientation of polymer chains and chain dis-entanglement in the amorphous content of the electrospun fibers should be both responsible for enhanced motion of polymer chain. It has been observed that while large diameter electrospun semi-crystalline polymer fibers are comprised of densely packed, misaligned lamellar structures connected by amorphous tie molecules, smaller diameter fibers consist of a fibrillar structure with alternating crystallites and extended amorphous tie molecules.[12] This is somewhat similar to the structure of the Nylon-11 nanofibers in this study, which were found to have increased crystallite orientation and size as well as increased orientation and confinement of connecting amorphous tie molecule regions (see supplementary material: X-ray scattering structural analysis), but no diameter-dependent change in fiber crystallinity (which was a constant ~36%).[14]

Recent studies have also indicated the formation of a core-shell structure in electrospun fibers caused by quick solvent evaporation at the fiber surface during the electrospinning process, which leads the polymer matrix to solidify in a

[a)]Electronic addresses: rkchen@ucsd.edu and shqcai@ucsd.edu

non-equilibrium state.[16,29–31] It has also been found that the electrospinning process creates a preferred orientation for polymer chains in the shell layer, whose thickness is independent of fiber diameter,[29] and prevents polymer chain relaxation, leaving them in a partially disentangled state.[30–32] We believe that those size-dependent molecular structures discussed above may also contribute to the strong size-dependent stress relaxation in the electrospun polymer nanofibers observed in our experiments. We would like to point out that more detailed analyses are needed to determine the accurate mechanisms responsible for such strong and unambiguous size-dependent stress relaxation in the nanofibers.

Herein we report, for the first time, significant size-dependent stress relaxation in semi-crystalline electrospun polymer (Nylon-11) nanofibers. In addition to increased stress relaxation upon diameter reduction, its associated time constant does not change as fiber diameter reduces below 200 nm, indicating that the viscosity of the relaxing constituents increases with further size reduction. Furthermore, the strong size-dependent stress relaxation in combination with the dramatically increasing stiffness indicates that electrospun nanofibers are ideal candidates for developing materials with simultaneously high stiffness and large damping capacity, a combination that is often difficult to find in natural and man-made materials.

II. EXPERIMENT METHODS

In the experiment, Nylon-11 nanofibers with different diameters were fabricated using the electrospinning technique as described in a previous paper.[14] To reveal the microstructure of semi-crystalline Nylon-11 nanofibers, we conducted small-angle X-ray scattering tests (SAXS) and the results are shown in supplementary material, Figure S1. The schematic of the microstructure of the nanofibers is shown in Figure 1(a). In the mechanical testing, individual Nylon-11 nanofibers were picked up with a micromanipulator in SEM and attached to the free end of an AFM cantilever with electron beam deposited Pt to conduct tensile measurements (Figure 1(b)). Each fiber was then pulled, causing the AFM cantilever to deflect and stress the fiber, where the applied force is directly related to the cantilever deflection and spring constant. Detailed experimental procedures are described as follows.

A. Cantilever calibration

The stress measurement requires both the fiber diameter and cantilever spring constant, which were both measured prior to the tensile measurement. The fiber geometry can easily be measured using low power SEM.[33] To extract the force applied to the fiber, spring constants for the AFM cantilevers were first calculated using the Sader method,[34,35] which requires the resonant properties of the cantilever since the spring constant of a rectangular cantilever is dependent on the cantilever geometry, material, and fundamental radial resonant frequency in a vacuum. We calculated this constant using the density and thickness of the cantilevers under the condition of cantilever length ≫ width ≫ thickness. Since the fundamental vacuum frequency shifts when the cantilever

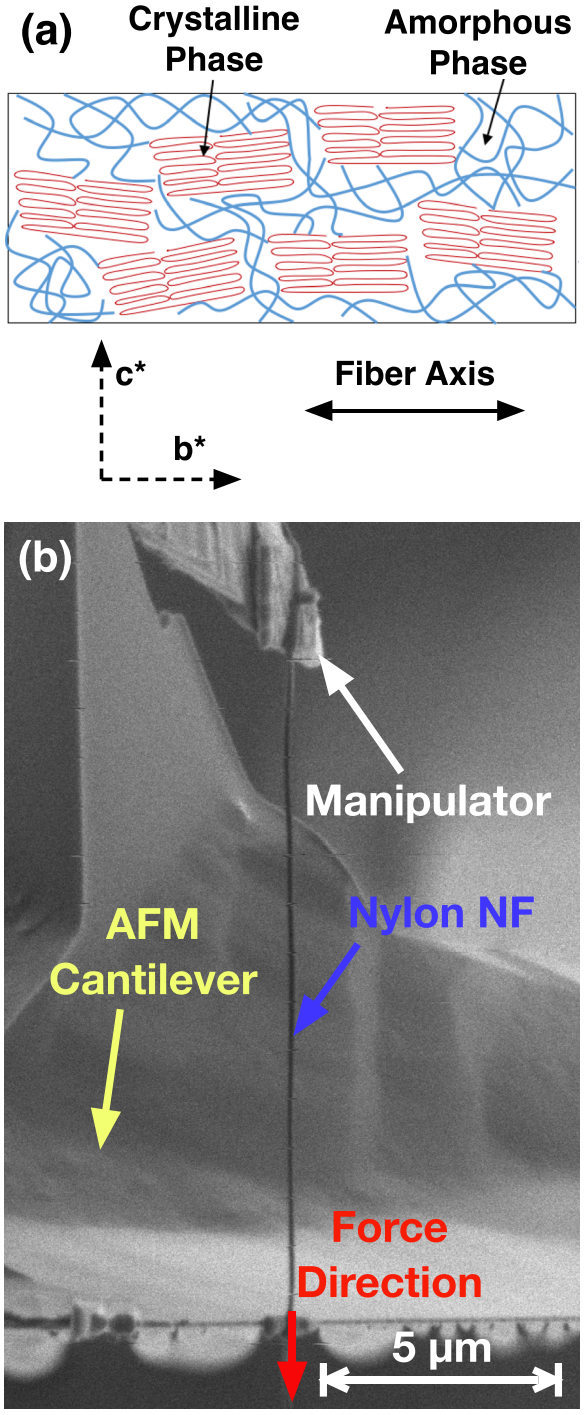

FIG. 1. (a) Schematic of the microstructure of semi-crystalline Nylon-11 nanofibers, consisting of crystalline and amorphous domains. (b) Single nanofiber tensile relaxation measurement setup: individual nanofibers were attached to AFM cantilevers *via* a tungsten manipulator in a dual-beam FIB. The fibers were pulled with the manipulator and both cantilever deflection and fiber length were monitored to measure applied stress and fiber strain.

is in a fluid, such as air, we can back out the vacuum frequency from that of the fluid shifted frequency by using the properties of the fluid. Then, with the cantilever width, the fluid hydrodynamic function, and the measured resonant quality factor in the fluid (which should be ≫1), the spring constant can be calculated. These resonant properties can be measured with either a laser vibrometer or an AFM. The cantilever undergoes an applied frequency sweep to measure the

resonance spectrum, where a narrower sweep band around the peak is identified and scanned to capture both the fluid resonance frequency and the quality factor. These parameters were then used to calculate the static spring constant.

B. Nanofiber tensile testing

Tensile testing of polymer fibers was performed in a SEM to image the length extension while using an AFM cantilever to apply and measure force along the fiber axial direction, similar to elasticity tests performed on nanowires and nanotubes.[36,37] Polymer fiber samples were attached to a tungsten probe in an SEM (FEI Scios Dualbeam) with electron beam deposited Pt (using an electron beam current of 0.4 nA at an accelerating voltage of 1.5 kV) and lifted from the substrates they were electrospun onto. The free ends of the fiber were then attached to the free end of an AFM cantilever and secured in place also with electron beam deposited Pt (the same deposition conditions). The manipulator probe was then used to pull the fiber and the cantilever deflection and fiber length were both measured with good accuracy by SEM (beam energies of ~1–1.5 kV were used for imaging so as not to damage the polymer).[33] The AFM cantilever deflection (supplementary material, Figure S2) and measured cantilever spring constant were used to calculate the force applied to the fiber. Fiber length measurements, taken at each measured cantilever deflection position (supplementary material, Figure S2), were used to calculate the strain on the fiber at each applied force. A stress-strain curve was then generated. The instantaneous tensile modulus, E_{inst}, of the fiber was measured based on the slope of consecutive stress and strain measurements (measured within ~1 min) and well within the linear extent of the stress-strain curve (supplementary material, Figure S3). Two different AFM cantilevers (with spring constants of 0.6 N m^{-1} and 5 N m^{-1}) were used to measure E_{inst} of the fibers and the resulting moduli were in good agreement with one another.

C. Nanofiber stress relaxation measurement

Stress relaxation on single Nylon-11 nanofibers was measured using a similar setup to that of the elastic modulus measurement. Single nanofibers were also lifted from substrates with a tungsten micromanipulator and the free end attached to a 5 N m^{-1} AFM cantilever. The nanofiber was then loaded to a set strain value. Measurements were done over a range of strains, 1.5%–7%, to check for strain dependence (see supplementary material, Table S1) with applied forces on the order of micro-Newtons (supplementary material, Figure S4). Cantilever deflection was measured every 5 to 10 min over a 2-h period. Relaxed tensile moduli, E_e, were calculated based on the final applied stress after relaxation ceased.

Because of the high stiffness of cantilever, the change of its deflection during the stress relaxation test is much smaller than the fiber elongation. Consequently, the tensile strain in the fiber is approximately a constant as required for standard stress relaxation test. In the experiment, no necking of the fibers was observed during the nanofiber relaxation tests. Relaxation measurements were also done on 50 nm Si nanowires, which showed no relaxation over the 2 h (see supplementary material, Figure S5), to confirm that stress relaxation was not caused by the cantilever itself. With no stress relaxation, changes in the cantilever deflection due to imaging resolution were shown to be less than ±2 nm (see supplementary material, Figure S6).

III. RESULTS AND DISCUSSION

A. Tensile moduli

Instantaneous and relaxed tensile moduli were measured for nanofibers with diameters ranging from 713 nm to 65 nm (Figure 2) and were found to both dramatically increase as fiber diameter decreased. This increase is similar to moduli previously measured in other polymer nanofibers upon size reduction[5,12,13,16,27,29,32,38] as well as in drawn polymer mats.[39] Fibers with diameters larger than ~400 nm exhibit moduli consistent with that of bulk Nylon-11,[40–42] ~0.6–1.5 GPa, whereas the thinner nanofibers had E_{inst} as high as 17.4 ± 2.3 GPa, respectively, which is a ~20-fold increase over the bulk value. A critical diameter of ~200 nm is observed for the onset of the sharp increase in the tensile modulus which is similar to the ~500 nm observed for Nylon-6,6,[43,44] compared to the lower ~50 nm for polypyrrole nanotubes[38] and higher ~800 nm for electrospun polystyrene.[45]

Interestingly, the relaxed moduli, E_e, exhibit a similar, albeit suppressed, increase as that of E_{inst} as fiber diameter is reduced demonstrating that some non-relaxing portion of the fiber contributes to the increased instantaneous tensile modulus. The deviation between E_{inst} and E_e indicates that the relaxing component of the fiber still accounts for an

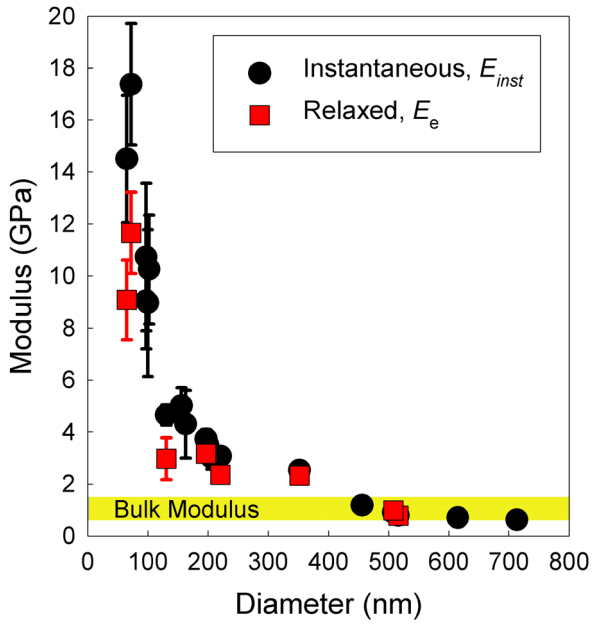

FIG. 2. Diameter dependence of instantaneous and relaxed moduli. While the elastic moduli of fibers with diameter >400 nm are bulk-like,[40–42] a dramatic increase occurs as the diameter drops below ~200 nm. The smallest nanofibers measured here, 65 and 72 nm, have instantaneous elastic moduli ~20 times larger than the bulk modulus. The relaxed moduli show two interesting phenomena: the degree of relaxation increases as the diameter decreases, but not down to bulk-like values, and dramatically increases as the diameter is reduced, similar to that of the instantaneous moduli.

appreciable amount of the enhanced stiffness, at least initially. It is known that at room temperature, Nylon-11 is a semi-crystalline polymer, in which stress relaxation mainly originates from its amorphous domain.[46] Our relaxation experiments elucidate the relative contributions of the crystalline and amorphous domains to the widely reported enhanced moduli in polymer nanofibers, in which only the initial moduli were often characterized.[5,12,13,16,27,29,32,38]

B. Stress relaxation

The size dependence of the relaxation leading to stiffness reduction was examined *via* stress relaxation behavior of fibers with diameters ranging from 516 nm to 65 nm over 2 h. The supported stress over time, as normalized by the initial stress, σ/σ_0, was found to significantly correlate with fiber diameter, as seen in Figure 3. For the ~500 nm diameter nanofibers, the largest diameter fiber studied here, no obvious stress relaxation was detected within the 2-h period. However, the amount of relaxation steadily increased as diameter decreased: σ/σ_0 for the 65 nm and 72 nm diameter fibers reduced to ~60% after only 20 min. Such stress relaxation is a well-known viscoelastic property of polymeric materials, though the relaxation we have observed in the smaller diameter fibers is comparatively fast for glassy polymers. We must note that though no obvious stress relaxation was seen in the largest diameter nanofibers, it is possible that they would follow a relaxation process similar to that of a bulk-like glassy polymer which would have taken a much longer time scale to observe than allowed in our current experimental setup.

C. Viscoelastic analysis

To quantitatively characterize the viscoelasticity of fibers and understand the implications of this strong size-dependent viscoelastic behavior, we analyzed the measured stress relaxation using a viscoelastic standard linear solid (SLS) model. In this model, the modulus is time dependent and follows $E(t) = E_e + E_r \cdot \exp(-t/\tau)$, where E_e and E_r are the elastic and relaxing contributions to the modulus, t is time, and τ is the relaxation time constant associated with the dissipative process. In our experiment, the tensile strain is a constant, so we can simply relate the transient modulus $E(t)$ of the fiber to the tensile stress $\sigma(t)$ as $\sigma(t)/\sigma_0 = E(t)/E_{inst}$, where σ_0 is the stress initially applied to the fiber and $E_{inst} = E(t=0)$. Furthermore, we can define a parameter β, relating our measured saturated stress relaxation to the moduli components, as $\beta = \lim_{t\to\infty} \sigma(t)/\sigma_0 = E_e/(E_e + E_r)$. The stress relaxation for the SLS model then follows $\sigma(t)/\sigma_0 = \beta + (1-\beta) \cdot \exp(-t/\tau)$, which has been fit to each nanofiber relaxation data set (shown as the solid lines in Figure 3). From this, we can define the amount of relaxation for each nanofiber as $1-\beta$ (Figure 4(a)), where the relaxation is approximately linearly correlated with the fiber diameter, compared to only a weak correlation with the initial applied stress (supplementary material, Figure S7).

1. Relaxation time constant

This stress relaxation fitting also allows us to extract the time constant, τ, related to the relaxation process for each measured fiber. Since no relaxation was observed for the ~500 nm diameter fibers, no time constant could be extracted; however, we do observe a decrease in τ as the diameter decreases and saturates below ~200 nm (Figure 4(b)), from ~14 min for the 352 nm diameter fiber to ~5 min for the remaining 65–221 nm diameter fibers. Based on these time constants, the viscosity (η) of the relaxing region of the fiber, related as $\eta = E_r \cdot \tau$, is initially constant down to ~200 nm. However, since τ is a constant for fibers below this size while the relaxing portion of the modulus (E_r) continues to increase, η should also increase as diameter is further reduced. This indicates that as the nanofibers are reduced in size, they will display a unique combination of high stiffness and large mechanical energy dissipation not present in their bulk form. It should be noted that it is highly possible that the relaxation time constant τ saturates at a larger diameter between 221 nm and 352 nm. Determination of the exact diameter where τ becomes a constant, however, is not a main target of our current study.

2. Stiffness and damping

From our viscoelastic stress relaxation model, we can define the ratio of the relaxing and elastic moduli

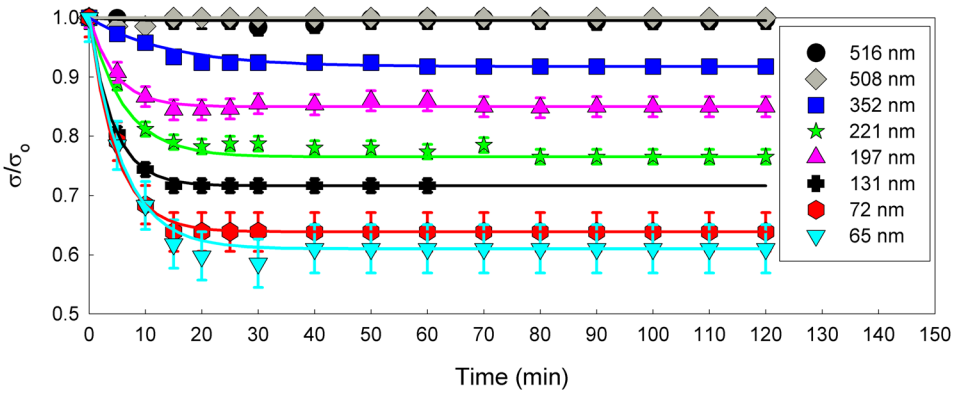

FIG. 3. Stress relaxation in individual Nylon-11 nanofibers. The time-dependent stress normalized by the initial stress, σ/σ_0, was measured over a 2-h period, with measurements taken every 5 to 10 min. Fibers of diameter ~500 nm show no relaxation over the measured time period; however, as diameter is reduced, stress relaxation increases, with stresses reduced to ~60% of the initial stress in the thinnest fibers. Legend lists nanofiber diameter for each relaxation measurement. Solid lines are fittings to the data based on a viscoelastic standard linear solid (SLS) model.

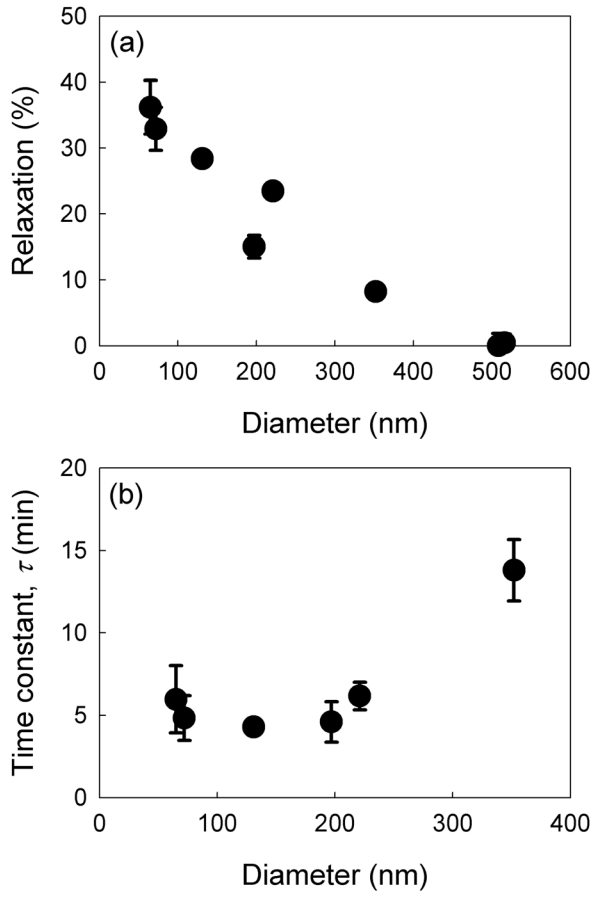

FIG. 4. Diameter dependent (a) stress relaxation and (b) relaxation time constant. The relaxation and time constants were calculated based on the fitting of a viscoelastic standard linear solid (SLS) model to the measured stress relaxation in Figure 3. (a) The degree of relaxation increases almost linearly with diameter reduction, starting from no observed relaxation in ~500 nm fibers and increasing up to ~40% for the thinnest measured fibers. (b) The relaxation time constant initially decreases with decreasing diameter down to ~200 nm, below which it saturates at ~5 min for all smaller diameters. Time constants could not be extracted from the ~500 nm diameter fibers as no relaxation was observed. The viscosity associated with the relaxing mechanisms of the fiber is initially constant down to ~200 nm and then, based on the saturated time constant and increasing relaxing component of the modulus, increases as the fiber diameter further decreases.

components as $\Delta = E_r/E_e = (1-\beta)/\beta$ and a maximum damping angle can be estimated as $\tan\delta = \Delta/(2\sqrt{1+\Delta})$, which represents the ratio of the viscous and elastic mechanical responses of the material and a measure of its capacity to dissipate mechanical energy.[47] As the diameters of the Nylon-11 nanofibers are reduced, the damping capacity significantly increases by a factor of ~100 (Figure 5) and while the damping is initially small, similar to metals, it increases even beyond that of other polymeric materials to levels comparable to the best recently developed composite materials.[48] It is important to note that the damping in the polymer nanofibers was measured at *room* temperature, whereas the high performance of the composites is achieved only at elevated temperature and performance decreases drastically as the operating temperature falls from 57 °C to 40 °C (and would most likely fall further if operated at 25 °C).

The specific modulus also increases from polymer-like to near metallic levels due to the higher strength to density

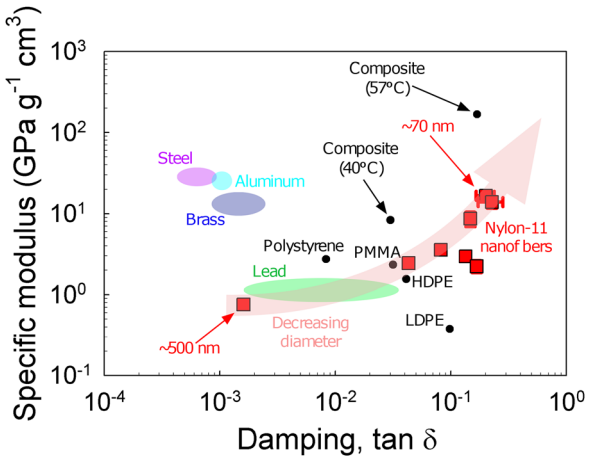

FIG. 5. Specific modulus versus maximum damping capacity (maximum tan δ). The specific modulus and damping capacity of the Nylon-11 nanofibers, calculated based on the measured tensile moduli and stress relaxation, are compared to those of other polymeric and metallic materials,[47] as well as a state-of-the-art composite[48] material. Both damping and specific modulus significantly increase by over an order of magnitude as fiber diameter is reduced, rising from low polymeric damping levels for ~500 nm diameter fibers to an impressive combination of specific modulus, comparable to the best structural metals, and damping capacity above that of many other polymers as fiber diameters are reduced below 100 nm. The thinnest fibers are even comparable to a state-of-the-art composite material.[48] The nanofibers, however, are operational at room temperature, whereas the composite performs best at elevated temperature and its performance quickly degrades as temperature drops.

ratios. This propels the nanofibers towards simultaneously high stiffness and damping, as compared to most materials, which is uncommon and highly suitable for applications involving vibration damping.[47] This property combination is realized using both un-optimized material and un-optimized operation conditions and better performance could be realized by changing the polymer and operating conditions (temperature, frequency, etc.). This is the first observation that nano-scaling of polymers, specifically fibers, could produce a new set of materials, tunable *via* size alone, with simultaneously high stiffness and large mechanical energy dissipation which would be highly desirable and useful. Last, we would like to point out that in many applications fibrous structures instead of individual electrospun polymer fibers will be adopted. Stiffness and damping capacity of fibrous structure generally depend on both the mechanical properties of individual fibers and their interactions. Additional characterizations of fibrous structures are imperative for their applications.

IV. CONCLUDING REMARKS

While size-dependent behavior of polymer nanofibers has been previously studied for several polymer systems, time-dependent mechanical properties of individual nanofibers have been paid little to no attention even though they are important aspects of polymer mechanics due to their viscoelastic nature. Here, we performed size-dependent tensile elastic and relaxation tests on semi-crystalline Nylon-11 nanofibers and found that stress relaxation in individual fibers is highly size-dependent, increasing significantly as diameter is reduced. The observed strong relaxation of

~40% occurs rapidly, saturating within ~30 min for the smallest nanofibers, which emphasizes the importance of considering the relaxed modulus when designing mechanical systems incorporating nanofibers, such as piezoelectric based devices[49] and nano-generators.[50–52] Furthermore, we found that the combination of significantly increasing relaxation and modulus upon size reduction leads to nanofibers with exceptionally high stiffness and mechanical energy damping properties, comparable to state-of-the-art composite materials, but operational at room temperature. This suggests that polymer nanofibers could be ideal candidates and provide substantially enhanced performance for applications which involve energy absorption, require toughness and flexibility, as artificial tissues such as skin, or in protective garments.

SUPPLEMENTARY MATERIAL

See supplementary material for additional experimental details of the article.

ACKNOWLEDGMENTS

This work was supported by National Science Foundation (DMR-1508420). FIB work was performed in Nano3 cleanroom at UCSD, a CALIT-2 facility. We thank FEI Company and Dr. B. Fruhberger and R. Anderson of Nano3 for the support and assistance on FIB. This research also used resources of the Advanced Photon Source, a U.S. Department of Energy (DOE) Office of Science User Facility operated for the DOE Office of Science by Argonne National Laboratory under Contract No. DE-AC02-06CH11357.

[1]Z. M. Huang, Y. Z. Zhang, M. Kotaki, and S. Ramakrishna, Compos. Sci. Technol. **63**, 2223 (2003).
[2]Y. Dzenis, Science **304**, 1917 (2004).
[3]D. Aussawasathien, J. H. Dong, and L. Dai, Synth. Met. **154**, 37 (2005).
[4]A. Frenot and I. S. Chronakis, Curr. Opin. Colloid Interface Sci. **8**, 64 (2003).
[5]A. Arinstein, M. Burman, O. Gendelman, and E. Zussman, Nat. Nanotechnol. **2**, 59 (2007).
[6]S. Shen, A. Henry, J. Tong, R. T. Zheng, and G. Chen, Nat. Nanotechnol. **5**, 251 (2010).
[7]S. Y. Chew, T. C. Hufnagel, C. T. Lim, and K. W. Leong, Nanotechnology **17**, 3880 (2006).
[8]M. Richard-Lacroix and C. Pellerin, Macromolecules **46**, 9473 (2013).
[9]M. Naraghi, P. V. Kolluru, and I. Chasiotis, J. Mech. Phys. Solids **62**, 257 (2014).
[10]A. Arinstein, J. Polym. Sci., Part B: Polym. Phys. **51**, 756 (2013).
[11]A. Baji, Y.-W. Mai, S.-C. Wong, M. Abtahi, and P. Chen, Compos. Sci. Technol. **70**, 703 (2010).
[12]C. T. Lim, E. P. S. Tan, and S. Y. Ng, Appl. Phys. Lett. **92**, 141908 (2008).
[13]D. Papkov, Y. Zou, M. N. Andalib, A. Goponenko, S. Z. D. Cheng, and Y. A. Dzenis, ACS Nano **7**, 3324 (2013).
[14]Z. Zhong, M. C. Wingert, J. Strzalka, H.-H. Wang, T. Sun, J. Wang, R. Chen, and Z. Jiang, Nanoscale **6**, 8283 (2014).
[15]W. Wang and A. H. Barber, J. Polym. Sci., Part B: Polym. Phys. **50**, 546 (2012).
[16]Y. Liu, S. Chen, E. Zussman, C. S. Korach, W. Zhao, and M. Rafailovich, Macromolecules **44**, 4439 (2011).
[17]R. O. Ritchie, Nat. Mater. **10**, 817 (2011).
[18]H. Schreuder-Gibson, P. Gibson, K. Senecal, M. Sennett, J. Walker, W. Yeomans, D. Ziegler, and P. P. Tsai, J. Adv. Mater. **34**, 44 (2002).
[19]S. J. Kwoun, R. M. Lec, B. H. Han, and F. K. Ko, in *Proceedings of the 2000 IEEE/EIA International Frequency Control Symposium & Exhibition* (2000), p. 52.
[20]Q. P. Pham, U. Sharma, and A. G. Mikos, Tissue Eng. **12**, 1197 (2006).
[21]B. K. Gu, M. S. Kim, C. M. Kang, J. I. Kim, S. J. Park, and C. H. Kim, J. Nanosci. Nanotechnol. **14**, 7621 (2014).
[22]V. Beachley, E. Katsanevakis, N. Zhang, and X. J. Wen, Biomed. Appl. Polym. Nanofibers **246**, 171 (2011).
[23]V. Singh, T. L. Bougher, A. Weathers, Y. Cai, K. Bi, M. T. Pettes, S. A. McMenamin, W. Lv, D. P. Resler, T. R. Gattuso, D. H. Altman, K. H. Sandhage, L. Shi, A. Henry, and B. A. Cola, Nat. Nanotechnol. **9**, 384 (2014).
[24]J. G. Williams, Polym. Eng. Sci. **17**, 144 (1977).
[25]R. S. Rivlin and A. G. Thomas, J. Polym. Sci. **10**, 291 (1953).
[26]W. Wang, A. J. Bushby, and A. H. Barber, Appl. Phys. Lett. **93**, 201907 (2008).
[27]M. Burman, A. Arinstein, and E. Zussman, Europhys. Lett. **96**, 16006 (2011).
[28]A. Arinstein, Y. Liu, M. Rafailovich, and E. Zussman, Europhys. Lett. **93**, 46001 (2011).
[29]U. Stachewicz, R. J. Bailey, W. Wang, and A. H. Barber, Polymer **53**, 5132 (2012).
[30]M. Richard-Lacroix and C. Pellerin, Macromolecules **48**, 4511 (2015).
[31]M. Richard-Lacroix and C. Pellerin, Macromolecules **48**, 37 (2015).
[32]Y. Ji, C. Li, G. Wang, J. Koo, S. Ge, B. Li, J. Jiang, B. Herzberg, T. Klein, S. Chen, J. C. Sokolov, and M. H. Rafailovich, Europhys. Lett. **84**, 56002 (2008).
[33]D. L. Vezie, E. L. Thomas, and W. W. Adams, Polymer **36**, 1761 (1995).
[34]J. E. Sader, J. W. M. Chon, and P. Mulvaney, Rev. Sci. Instrum. **70**, 3967 (1999).
[35]J. E. Sader, J. A. Sanelli, B. D. Adamson, J. P. Monty, X. Z. Wei, S. A. Crawford, J. R. Friend, I. Marusic, P. Mulvaney, and E. J. Bieske, Rev. Sci. Instrum. **83**, 103705 (2012).
[36]Y. Zhu, F. Xu, Q. Q. Qin, W. Y. Fung, and W. Lu, Nano Lett. **9**, 3934 (2009).
[37]M. C. Wingert, S. Kwon, M. Hu, D. Poulikakos, J. Xiang, and R. Chen, Nano Lett. **15**, 2605 (2015).
[38]S. Cuenot, S. Demoustier-Champagne, and B. Nysten, Phys. Rev. Lett. **85**, 1690 (2000).
[39]C. L. Choy, Y. W. Wong, G. W. Yang, and T. Kanamoto, J. Polym. Sci., Part B: Polym. Phys. **37**, 3359 (1999).
[40]Y. C. Hu, L. Shen, H. Yang, M. Wang, T. X. Liu, T. Liang, and J. Zhang, Polym. Test. **25**, 492 (2006).
[41]E. Petrovicova, R. Knight, L. S. Schadler, and T. E. Twardowski, J. Appl. Polym. Sci. **78**, 2272 (2000).
[42]H. Chung and S. Das, Mater. Sci. Eng. A **437**, 226 (2006).
[43]E. Zussman, M. Burman, A. L. Yarin, R. Khalfin, and Y. Cohen, J. Polym. Sci. B **44**, 1482 (2006).
[44]M. Burman, A. Arinstein, and E. Zussman, Appl. Phys. Lett. **93**, 193118 (2008).
[45]Y. Ji, B. Li, S. Ge, J. C. Sokolov, and M. H. Rafailovich, Langmuir **22**, 1321 (2006).
[46]K. Hong, A. Rastogi, and G. Strobl, Macromolecules **37**, 10174 (2004).
[47]R. Lakes, *Viscoelastic Materials* (Cambridge University Press, 2009).
[48]T. Jaglinski, D. Kochmann, D. Stone, and R. S. Lakes, Science **315**, 620 (2007).
[49]L. Persano, C. Dagdeviren, Y. Su, Y. Zhang, S. Girardo, D. Pisignano, Y. Huang, and J. A. Rogers, Nat. Commun. **4**, 1633 (2013).
[50]J. Chang, M. Dommer, C. Chang, and L. Lin, Nano Energy **1**, 356 (2012).
[51]C. Chang, V. H. Tran, J. Wang, Y.-K. Fuh, and L. Lin, Nano Lett. **10**, 726 (2010).
[52]B. J. Hansen, Y. Liu, R. Yang, and Z. L. Wang, ACS Nano **4**, 3647 (2010).

Supplementary Information:

Strong Size-dependent Stress Relaxation in Polymer Nanofibers

Matthew C. Wingert[a], Zhang Jiang[b], Renkun Chen[a], Shengqiang Cai[a]

[a]Department of Mechanical and Aerospace Engineering, University of California, San Diego, La Jolla, California 92093, USA

[b]X-ray Science Division, Argonne National Laboratory, Argonne, Illinois 60439, USA

X-ray scattering structural analysis

Detailed structural characterization of Nylon-11 nanofibers has previously been carried out by us using high-resolution wide-angle X-ray scattering (WAXS).[1] This X-ray analysis showed that the orientational order parameter increased as fiber diameter decreased, especially below ~400 nm. This increased ordering within the nanofibers comes from the decrease in the average crystal inclination angle upon shrinking fiber diameter, meaning the crystallites within the fibers were increasingly aligned along the fiber axis as diameter was reduced. Bulk Nylon-11, on the other hand, does not exhibit any preferred orientation. The crystallite size along the fiber axis was also shown to quickly increase when the nanofiber diameter shrank below ~200 nm, a similar critical size as seen from the perspectives of the thermal and mechanical properties. The crystallite size along the fiber axial direction was determined to be 10.5 ± 0.5 nm for ~200 nm nanofibers.[1] The crystallite size perpendicular to the fiber axis, however, was approximately constant. Furthermore, crystallinity of the nanofibers was nearly constant at 36% over the entire measured diameter range.

As fiber crystallinity is nearly constant while the crystallites elongate when the fiber diameter decreases, some crystalline lamellae must have merged to form larger crystals. This suggests that the average spacing between neighboring crystallites along the axial direction could have been decreased. To reveal this, we have utilized small-angle X-ray scattering (SAXS). As shown in Figure S1, from the fitting of the Lorentzian-shaped diffraction peak (0. 70 nm^{-1}), we can determine the spacing between neighboring crystallites along the axial direction to be about 9.0 nm for 200 nm nanofibers. Importantly, this spacing is very close to the (010) crystallite size determined from the WAXS experiment (10.5 ± 0.5 nm for ~200 nm nanofibers), which indicates that the crystallites are nearly in touch with each other along the axial direction.

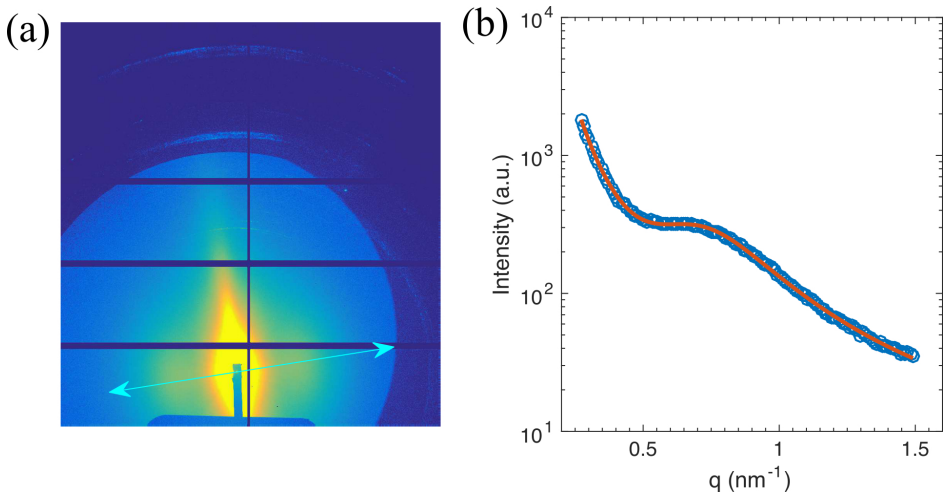

Supplementary Figure S1: Small-angle X-ray scattering (SAXS) results of ~200 nm diameter Nylon-11 nanofibers. (a) SAXS patterns from uniaxially aligned nanofibers of diameter of ~200 nm. (b) Intensity line (intensity vs. *q*) cuts along the (010) direction (b* axis), which is used to calculate the average distance between two neighbouring crystals among the fiber axis (determined to be 9.0 nm).

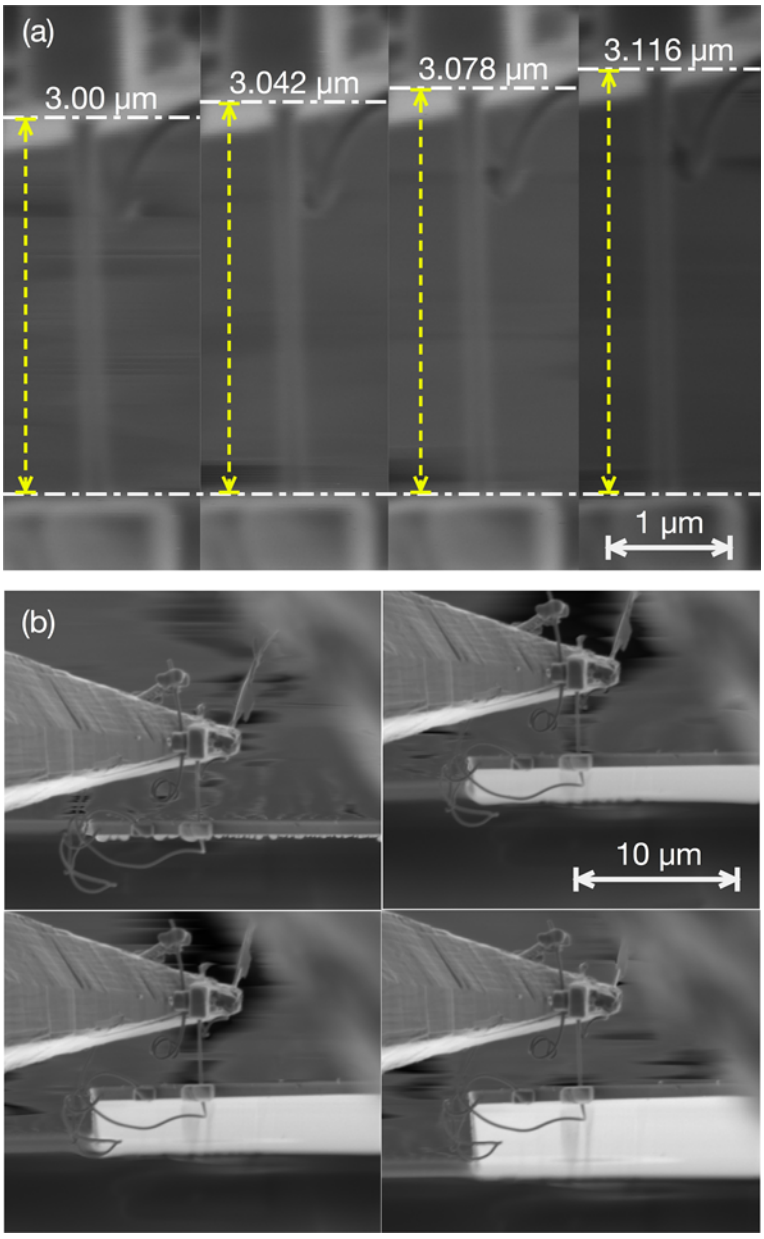

Supplementary Figure S2: (a) Nanofiber strain measurement. During each loading, in addition to the cantilever deflection, the fiber length is measured and converted to applied strain. (b) Cantilever deflection during elastic modulus measurement. The nanofiber is attached to the edge of an AFM cantilever and pulled. The measured deflection is converted to applied stress on the fiber for each loading step.

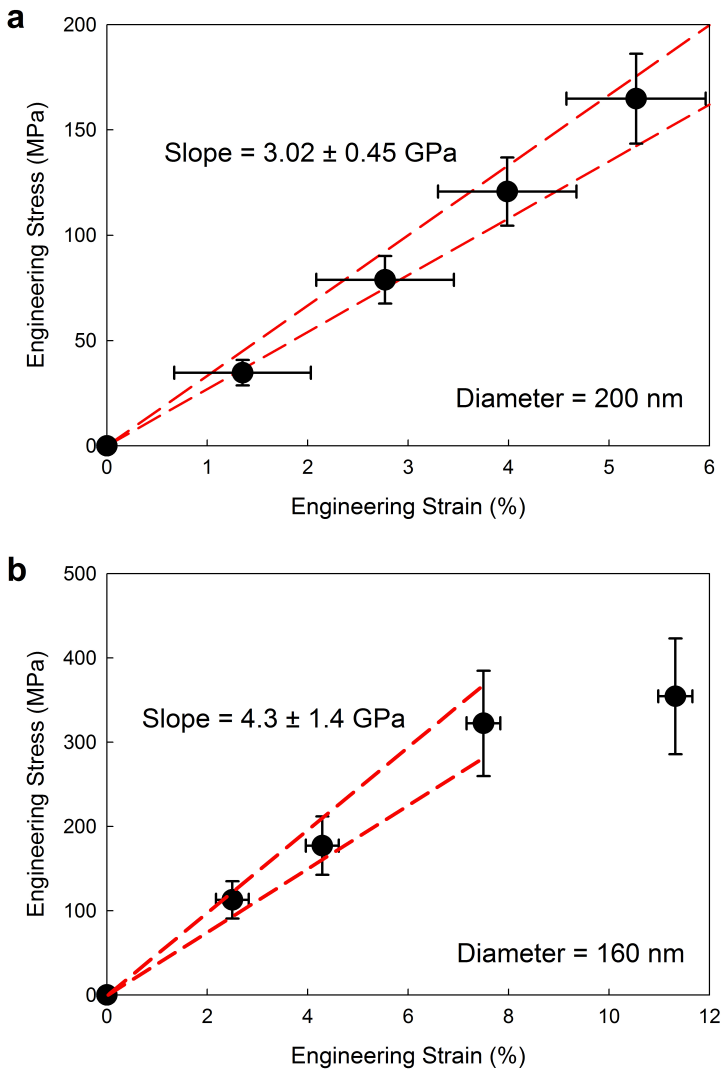

Supplementary Figure S3: Engineering stress-strain curve for single (a) ~200 nm and (b) ~160 nm diameter nanofibers. The measured cantilever deflection and fiber length are converted to stress and strain for each fiber. The slope of the linear portion of the stress-strain curve (usually less than 6-8% strain) is the nanofiber elastic modulus. Since the measurement was done quickly (within ~1 minute), the modulus can be considered instantaneous. Dashed red lines represent upper and lower bounds of the linear portion of the stress-strain curve, respectively.

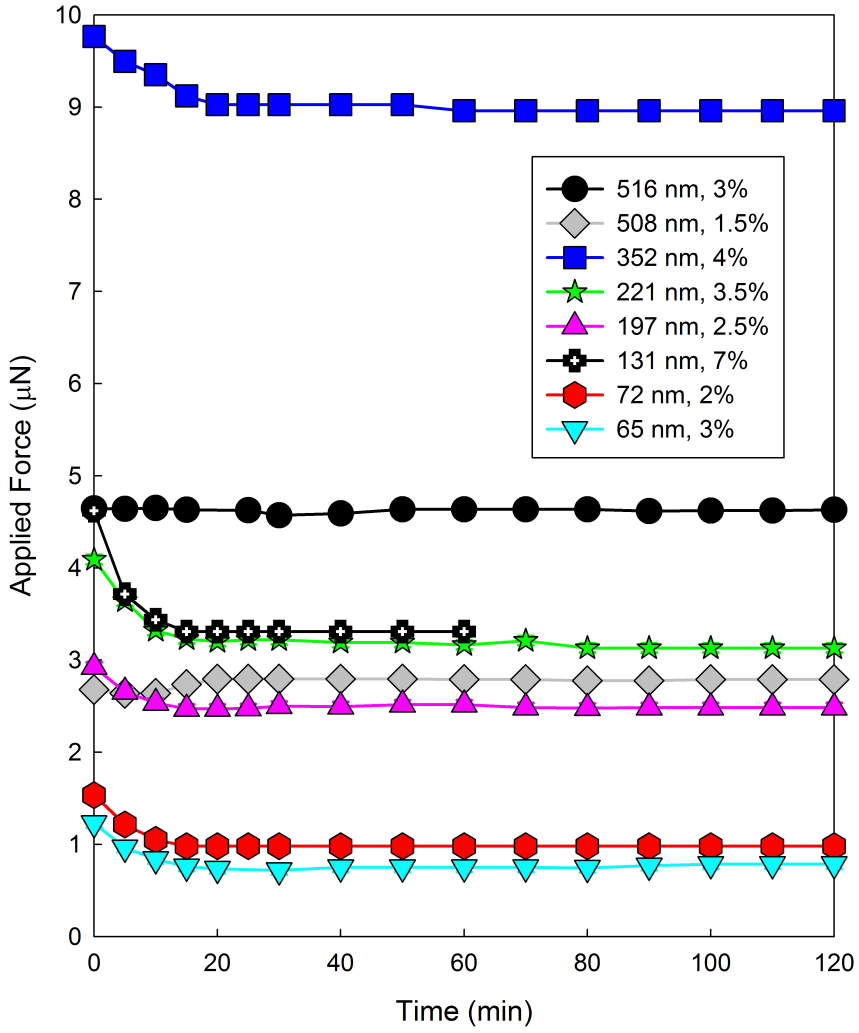

Supplementary Figure S4: Applied force during time-dependent relaxation tests. The applied force in all relaxation tests was on the order of μN. The degree of force relaxation is independent of initial applied force or strain on the fiber and depends only on the diameter of the nanofiber.

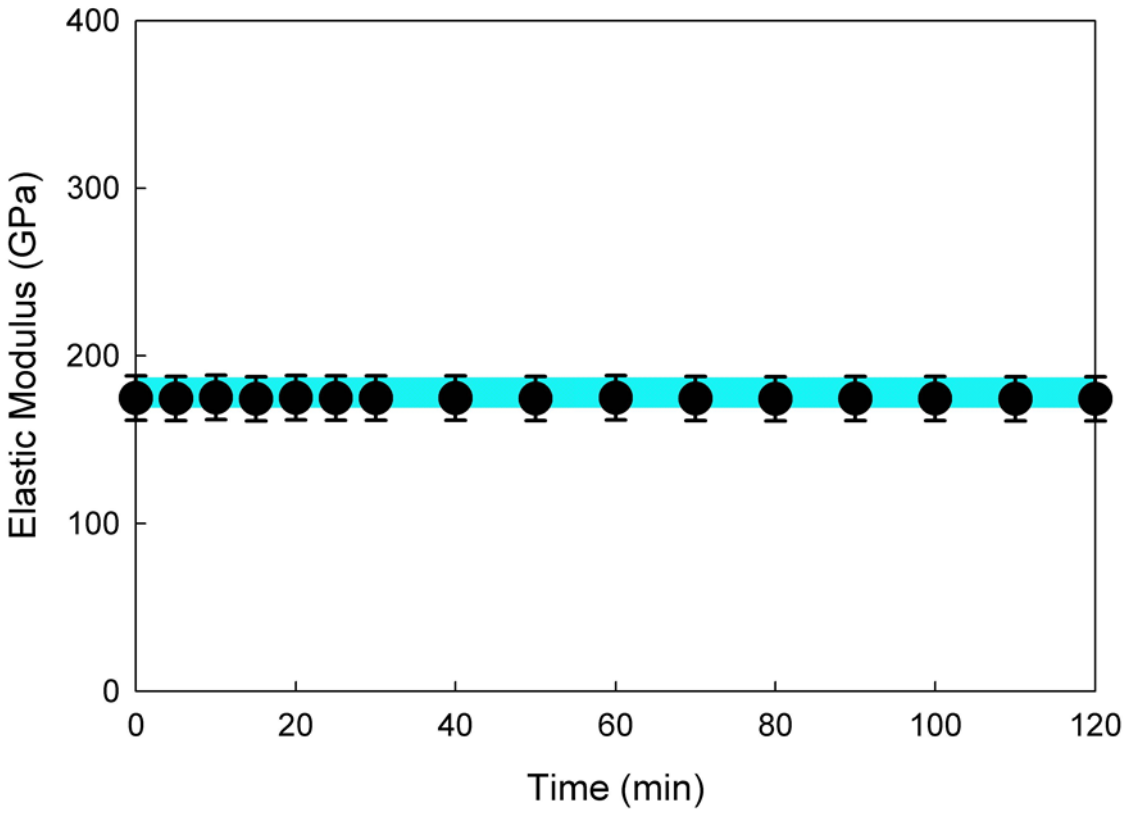

Supplementary Figure S5: Control relaxation test using a 50 nm diameter Si nanowire. The stress relaxation measurement was also done on a Si nanowire to rule out the possibility of the cantilever being the source of the measured stress relaxation. Since Si should not experience any relaxation, just such expected behavior is observed and the modulus consistent with bulk Si (blue band).[2]

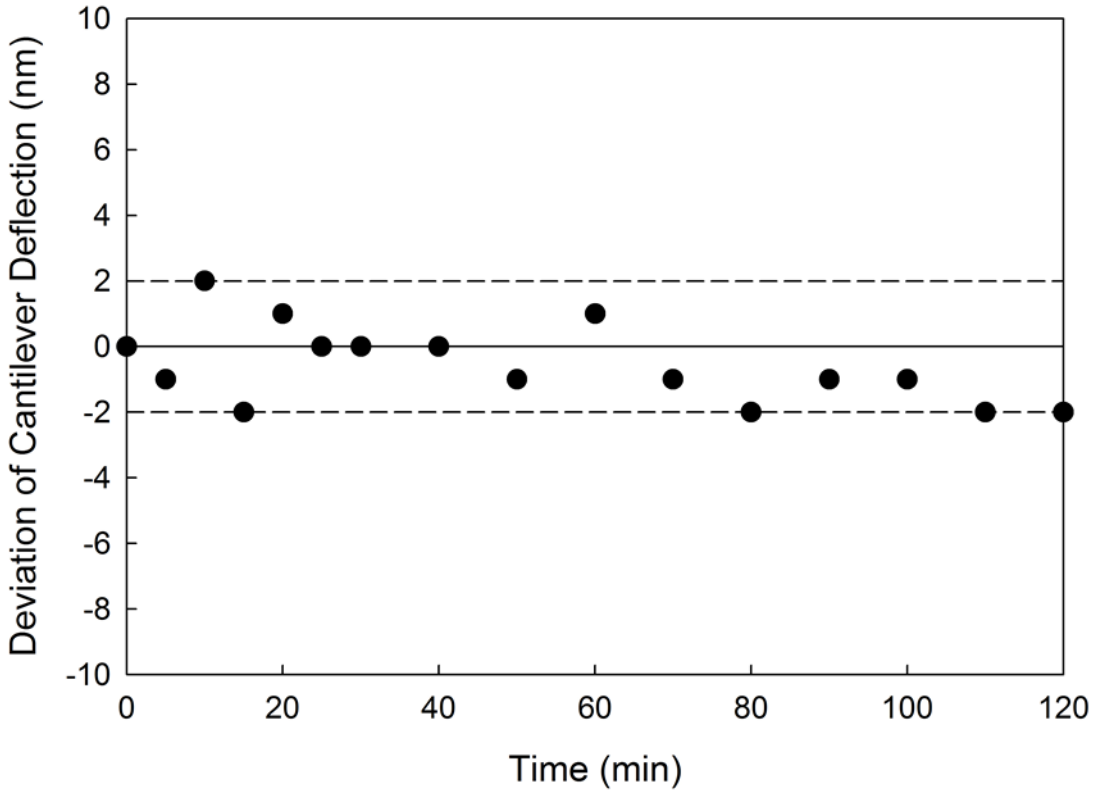

Supplementary Figure S6: Deviation of the cantilever deflection during Si nanowire stress relaxation test. The cantilever deflection is approximately constant over the measured time period indicating no stress relaxation from the cantilever itself.

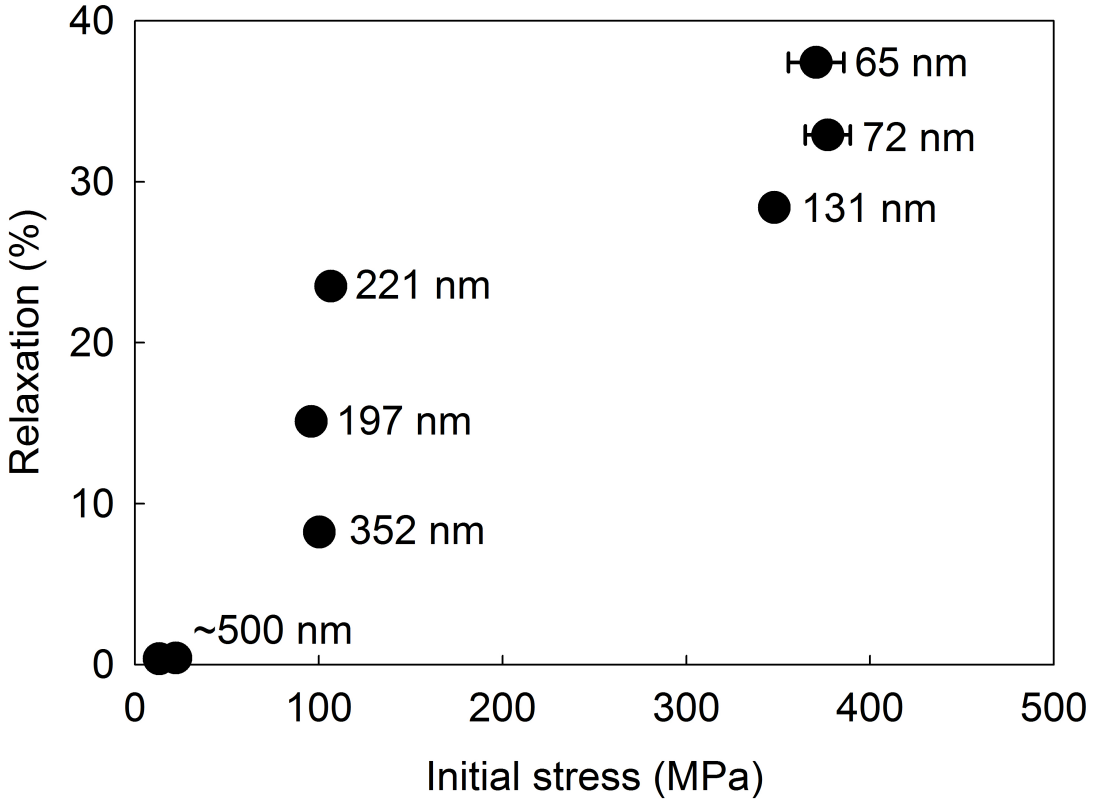

Supplementary Figure S7: Full stress relaxation versus initial applied stress. The amount of relaxation is strongly dependent on the diameter of the nanofiber and not on the initial applied stress or strain. Data points are labeled by fiber diameter.

Supplementary Table S1: Nanofiber relaxation conditions and measured properties

D (nm)	σ_o (MPa)	ε_o (%)	Relaxation (%)	E_{inst} (GPa)	τ (min)
516	23.7	3	0.43	0.79	N/A
508	13.7	1.5	0.36	0.91	N/A
352	101.6	4	8.24	2.54	13.8
221	107.5	3.5	23.5	3.07	6.17
197	93.0	2.5	15.0	3.72	4.60
131	348.0	7	28.4	4.65	4.29
72	346.0	2	32.9	17.3	4.83
65	435.0	3	36.2	14.5	5.97

References:

1. Zhong, Z.; Wingert, M. C.; Strzalka, J.; Wang, H.-H.; Sun, T.; Wang, J.; Chen, R.; Jiang, Z. *Nanoscale* **2014,** 6, (14), 8283-8291.
2. Zhu, Y.; Xu, F.; Qin, Q. Q.; Fung, W. Y.; Lu, W. *Nano Letters* **2009,** 9, (11), 3934-3939.